

Effect of Strain Rate on Compressive Properties of Aluminium-Graphene Composites

Yufu Yan ¹, Jiamin Zhao ¹, Long Chen ¹, Hongjian Zhao ¹, Olga Klimova-Korsmik ², Oleg V. Tolochko ^{2,3}, Fuxing Yin ⁴, Puguang Ji ^{1,2,*} and Shaoming Kang ^{1,*}

¹ School of Materials Science & Engineering and Tianjin Key Laboratory of Materials Laminating Fabrication and Interface Control Technology, Hebei University of Technology, Tianjin 300130, China

² World-Class Research Center “Advanced Digital Technologies”, State Marine Technical University, Saint Petersburg 190121, Russia

³ Institute of Mechanical Manufacturing, Materials, and Transportation, Peter the Great St. Petersburg Polytechnic University, Saint Petersburg 195251, Russia

⁴ Institute of New Materials, Guangdong Academy of Sciences, Guangzhou 510651, China

* Correspondence: jipuguang@hebut.edu.cn (P.J.); kangdashao@163.com (S.K.)

Abstract: Graphene-reinforced aluminium composites have been widely studied due to their excellent mechanical properties. However, only a few studies have reported their dynamic compression properties. The purpose of this study is to investigate the quasi-static and dynamic compression properties of graphene-reinforced aluminium composites. The addition of graphene improved the compressive stress resistance and energy absorption capacity of the aluminium matrix. An aluminium-0.5 wt.% graphene composite exhibited good compressive properties due to the different interfacial wave impedance generated by the additional grain boundaries or aluminium–graphene interfaces.

Keywords: aluminium matrix composite; graphene; quasi-static compression; dynamic compression; powder metallurgy



Citation: Yan, Y.; Zhao, J.; Chen, L.; Zhao, H.; Klimova-Korsmik, O.; Tolochko, O.V.; Yin, F.; Ji, P.; Kang, S. Effect of Strain Rate on Compressive Properties of Aluminium-Graphene Composites. *Metals* **2023**, *13*, 618. <https://doi.org/10.3390/met13030618>

Academic Editor: Emin Bayraktar

Received: 16 February 2023

Revised: 3 March 2023

Accepted: 8 March 2023

Published: 20 March 2023



Copyright: © 2023 by the authors. Licensee MDPI, Basel, Switzerland. This article is an open access article distributed under the terms and conditions of the Creative Commons Attribution (CC BY) license (<https://creativecommons.org/licenses/by/4.0/>).

1. Introduction

Aluminium and its alloys have been widely used in many fields, such as aerospace, military, industry, and transportation, owing to their low density, low melting point, and excellent mechanical and physical properties [1–3]. Aluminium matrix composites are a group of advanced materials with a high application potential in practical engineering applications [4,5]. Composites of aluminium and its alloys are prepared by doping with reinforcing phases (such as Al₂O₃ [6–8] and SiC [9–11]) to improve their mechanical properties. Since its appearance in 2004 [12,13], and due to its excellent properties, graphene has gradually replaced Al₂O₃ and SiC as reinforcing phases to improve the mechanical properties of aluminium matrix composites [14–16]. In practical engineering applications, materials are often subjected to dynamic and quasi-static loads. The dynamic properties of materials are important as they affect the service life of components.

Many researchers have studied the dynamic compressive properties of aluminium and its composites with reinforced phases. For instance, Zaiemyekheh et al. [17] investigated the quasi-static and dynamic behaviours of aluminium composites reinforced with different weight percentages of Al₂O₃. They found that the addition of 5.0 wt.% Al₂O₃ significantly improved the compressive strength and energy absorption capacity of aluminium. Wang et al. [18] prepared carbon nanotube-reinforced aluminium matrix composites and investigated their compressive properties at different strain rates. Under the same test conditions, the best compressive properties were achieved when the carbon nanotube content was 2.0 wt.%. Wang et al. [19] prepared aluminium composites reinforced with glass microspheres by hot pressing and investigated their compressive properties at different pressures. They found that the composite hot-pressed at 15 MPa exhibited better

compression resistance. These studies indicate that the reinforced phase enhances the dynamic compressive properties of composites.

In recent years, graphene has been used as the reinforcement phase in aluminium matrices because of its high specific surface area, high ductility, and high tensile strength. Khanna et al. [20] prepared graphene-reinforced aluminium matrix composites and found that the compressive strength and hardness of the materials were highest when the graphene nanosheet content was 0.25 wt.%. Sharma et al. [21] prepared 0.3 wt.% graphene-reinforced aluminium matrix composites and found that the compressive strength and hardness increased by 23.61 and 24.65%, respectively, compared with those of pure aluminium. However, these studies focus only on the quasi-static performance of aluminium-graphene composites and do not report their dynamic compressive properties. Compared with foam aluminium with better dynamic compression performance [22,23], aluminium-graphene composite is more suitable for practical engineering applications.

In this study, aluminium-graphene composites were prepared with different graphene contents using powder metallurgy techniques. We studied their quasi-static and dynamic compressive properties at different strain rates.

2. Material and Methods

The raw materials consisted of high-purity (purity $\geq 99.9\%$) spherical aluminium powder with a particle size of 1–2 μm and monolayer graphene (99.9% purity) oxide in aqueous solution. Aqueous solutions of graphene oxide with different mass fractions (0.5 and 1.0 wt.%) were mixed with the aluminium powder using a stirrer (speed: 300 r/min; duration: 2 h) to obtain graphene oxide–aluminium composite powders after freeze drying. The composite powders were then placed in a tube furnace and heated to 550 $^{\circ}\text{C}$ (atmosphere: hydrogen; duration: 2 h) for thermal reduction to graphene–aluminium composite powders. The reduced powders were loaded into a graphite mould and sintered in a vacuum hot press furnace. The sintering temperature, pressure, and duration were 600 $^{\circ}\text{C}$, 40 MPa, and 2 h, respectively. The preparation process is illustrated schematically in Figure 1.

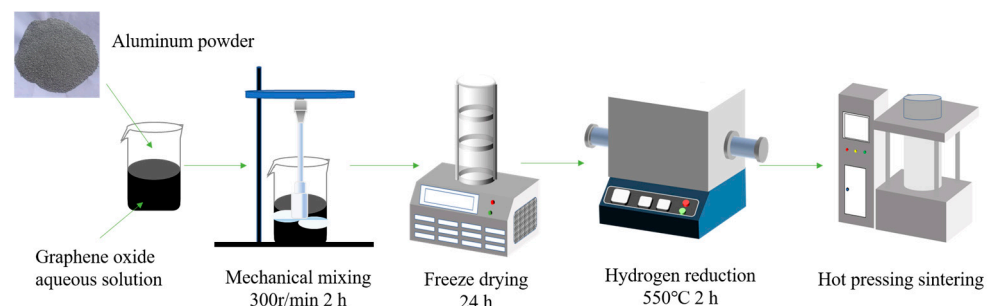


Figure 1. Preparation of aluminium-graphene composites.

The microstructures of the aluminium-graphene composites were determined via X-ray diffraction (Bruker D8-focus, $\lambda = 1.5406 \text{ \AA}$; the voltage and current were 40 kV and 40 mA), Raman spectroscopy (in-Via Reflex; the wavelength was 532 nm), and scanning electron microscopy (SEM, JEOL JSM-7100 F) techniques. Quasi-static compression tests (Electronic universal material testing machine, AGS-XD50kN, Shimadzu corporation, Kyoto, Japan) were carried out at room temperature (about 25 $^{\circ}\text{C}$) on cylindrical specimens (diameter: 10 mm; length: 20 mm; complying with the national standards of GB/T 7314-2017) at a speed of 1.2 mm/min and a crosshead separation rate of 10^{-3} /s. Hopkinson compression bar tests (separate Hopkinson press bar, SHPB-ALT1000, Archimedes Industrial Technology Ltd., Beijing, China) were conducted at strain rates of 2000, 3000, and 4000/s on specimens with a diameter and height of 8 mm, complying with the national standards of GB/T 34108-2017.

3. Results and Discussion

Figure 2 shows the SEM images, XRD patterns, and Raman spectra of the aluminium-graphene composites. Graphene flakes uniformly cover the surface of the aluminium spheres, as shown in Figure 2a,b. The XRD pattern (Figure 2c) shows peaks corresponding to aluminium; however, no characteristic peaks of graphene are observed. This is because the content of the graphene added is small, and graphene does not have the serious agglomeration phenomenon, which is beneficial to the performance of the subsequent composite materials [24]. The Raman spectrum of the composite (Figure 2d) shows the characteristic D and G peaks of graphene at ~ 1336 and ~ 1590 cm^{-1} , respectively. In general, the intensity ratio of the D and G peaks (ID/IG) indicates defects in the graphite structure. The calculated ID/IG ratios are 1.16 and 1.15 for the two composites (0.5 and 1.0 wt.% graphene, respectively), indicating that most of the graphene in the composite powder has a small number of defects, but this does not affect the later properties. Furthermore, the intensities of the Raman peaks increase with an increase in the graphene content.

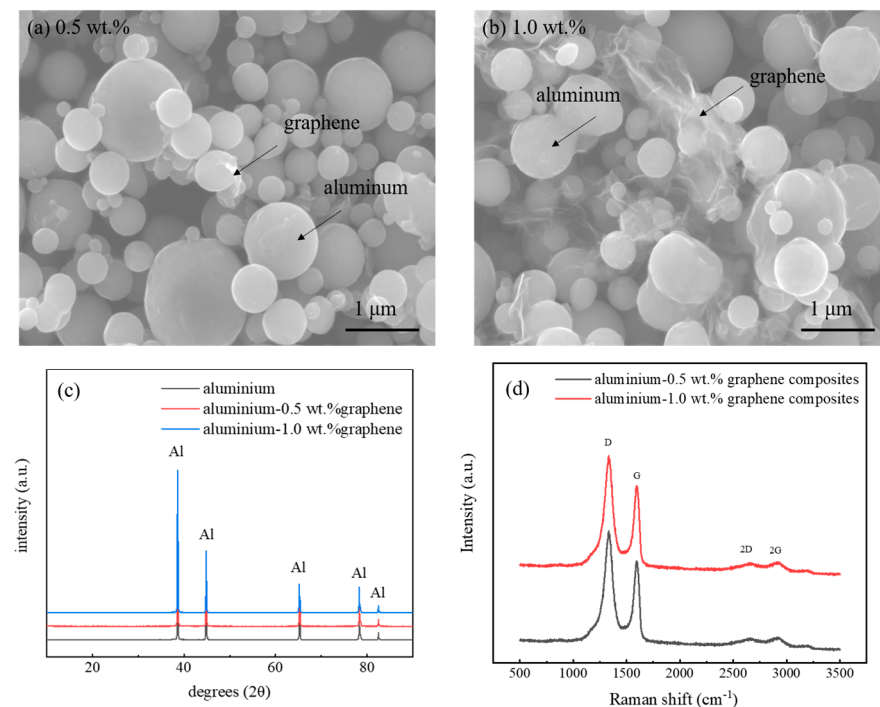


Figure 2. SEM images, XRD patterns, and Raman spectrum of aluminium-graphene powders. (a) SEM images of 0.5 wt.% aluminium-graphene powder; (b) SEM images of 1.0 wt.% aluminium-graphene powders; (c) XRD patterns of aluminium-graphene powders; (d) Raman spectrum of aluminium-graphene powders.

Figures 3 and 4 show the electron backscatter diffraction and electron microprobe analysis results of the aluminium-graphene composites. As shown in Figure 3, all the composites exhibit equiaxed grains. The sizes of the equiaxed grains decrease with an increase in the graphene content, indicating the presence of more grain boundaries. The elemental mapping (Figure 4) shows that the graphene is well distributed.

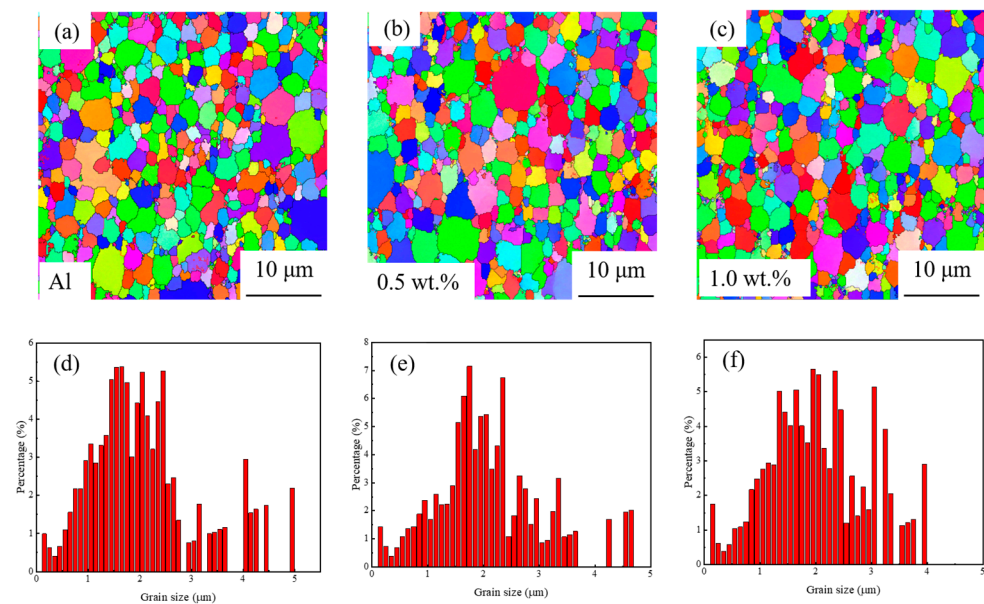


Figure 3. EBSD analysis of aluminium-graphene composites: (a–c) EBSD of aluminium-graphene composites; (d–f) grain size distribution map corresponding to (a–c), respectively.

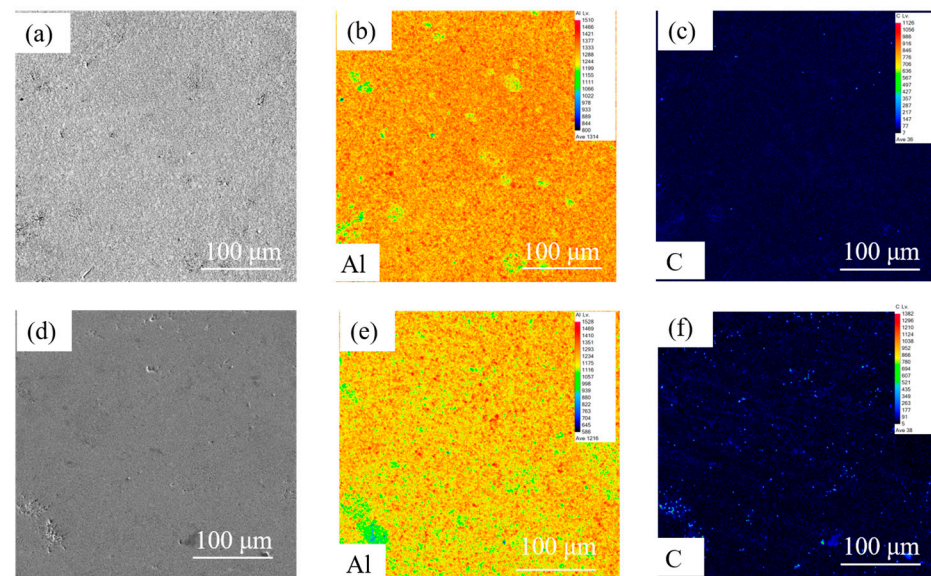


Figure 4. EPMA analysis of aluminium-graphene composites: (a–c) secondary electron image of aluminium-0.5 wt.% graphene composites and Al/C element distribution; (d–f) SEI of aluminium-1.0 wt.% graphene composites and Al/C element distribution.

Figures 5 and 6 show the stress–strain curves and stress variation of the aluminium-graphene composites under quasi-static and dynamic compression, respectively. In the quasi-static condition (Figure 5a), all the aluminium-graphene composites exhibit similar elastic deformation behaviours at strains below 0.04. The aluminium matrix shows a long plastic region with a constant stress plateau in the strain range of 0.04–0.5. After adding 0.5 wt.% graphene, the composite exhibits a plastic region in the strain range of 0.04–0.32, and the stress increases with an increase in the strain. With the addition of 1.0 wt.% graphene, the plastic region of the composite becomes shorter, and the stress shows a similar trend to that of the composite with 0.5 wt.% graphene. The peak compressive stresses of the aluminium-0.5 wt.% graphene and aluminium-1.0 wt.% graphene are 238 and 187 MPa, respectively, which are 40 and 10% higher than that of the aluminium matrix

(170 MPa), respectively. The increased stress and decreased strain indicate that the addition of graphene enhances the compressive strength of the aluminium matrix. In the dynamic compressive stress–strain curves (Figure 5b–d), the compressive stress first increases and then decreases with an increase in the graphene content (at the same strain rate). The peak compressive stresses of the aluminium-0.5 wt.% graphene are 286 ± 3 , 299 ± 5 , and 280 ± 1 MPa, respectively, at strain rates of 2000, 3000, and 4000/s, which are 13.9, 15.0, and 1.5% higher than those of the aluminium matrix, respectively. When the composite is subjected to an external force, the load is transferred from the low-strength aluminium to the high-performing graphene through the interface between aluminium and graphene, so that graphene replaces aluminium as the main load bearer and strengthens the compressive properties of the composite. At the same time, graphene as a fine second-phase particle interacts with dislocations and therefore effectively hinders their movement. Due to the large difference in thermal expansion coefficients between graphene and aluminium, a high dislocation density zone is formed around the graphene, creating a dislocation ring, which further enhances the compressive properties of the composite [24].

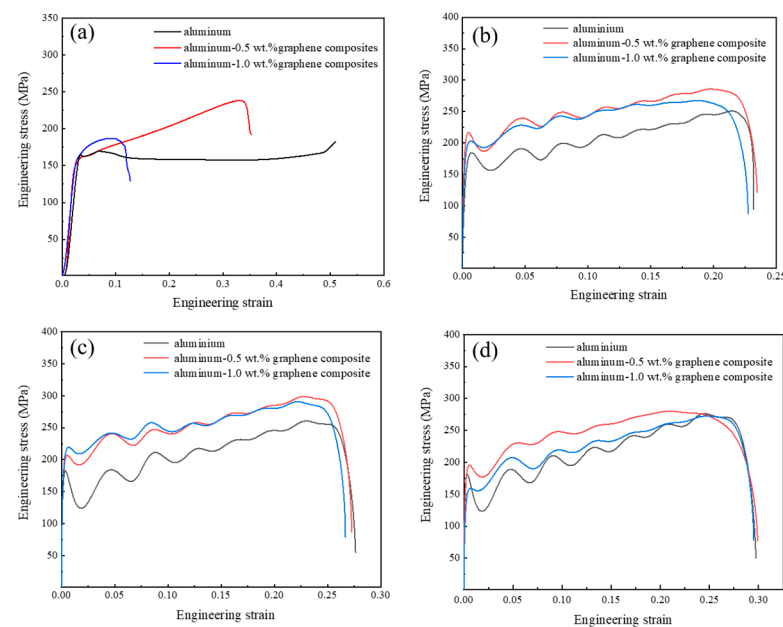


Figure 5. Stress–strain curves for quasi-static and dynamic compression of aluminium-graphene composites: (a) quasi-static; (b–d) dynamic compression with strain rates of 2000/s, 3000/s, and 4000/s, respectively.

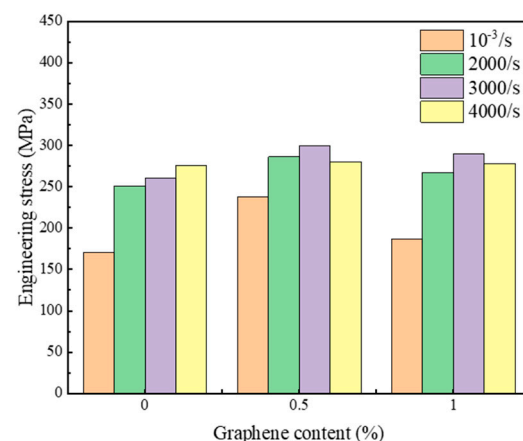


Figure 6. Stress variation diagram of aluminium-graphene composite under quasi-static and dynamic compression.

Figure 7a shows the energy absorption capacity of the aluminium-graphene composites. The absorbed energy is the area of the stress–strain curve derived by calculus from the test system carried by the Hopkinson press bar. At the same strain rate, the energy absorption capacity of the aluminium matrix increases with the addition of graphene, reaching a maximum value at 0.5 wt.%, and then decreases. The maximum energy absorption capacities are 23.35 ± 2.32 , 27.04 ± 1.89 , and 29.15 ± 2.18 J/cm³, respectively, at strain rates of 2000, 3000, and 4000/s. Thus, the energy absorption capacity of the composite increases with an increase in the strain rate. At the same strain rate, the incident waves entering the pure aluminium matrix are transmitted due to strong interface adhesion. We simulated the interface adhesion between graphene and aluminium based on the preparation process of the composite powder (Figure 7b). In the aluminium-0.5 wt.% graphene composite, most of the incident waves are reflected because of the impedance mismatch between aluminium and graphene interfaces. In addition, the presence of more grain boundaries can enhance the energy absorption capacity, whereas in the aluminium-1.0 wt.% graphene composite, the large amount of graphene present at the aluminium sphere interfaces destroys the bonding strength and decreases its energy absorption capacity. For example, in the more popular sandwich structure of the composite material [19], when the high-speed shock wave acts on the aluminium surface, it passes through the aluminium interface to the surface of the graphene structure, and then into the graphene, indicating reflection and transmission propagation, due to the difference in the content of the graphene. On part of the graphene surface, the transmitted wave is converted to a compressional wave, the reflected wave is converted to a stretching wave, and the transmitted propagated compressional wave will be reflected and transmitted at another aluminium interface. Repeated wave propagation occurs, and this process leads to wave impedance at both of the interfaces.

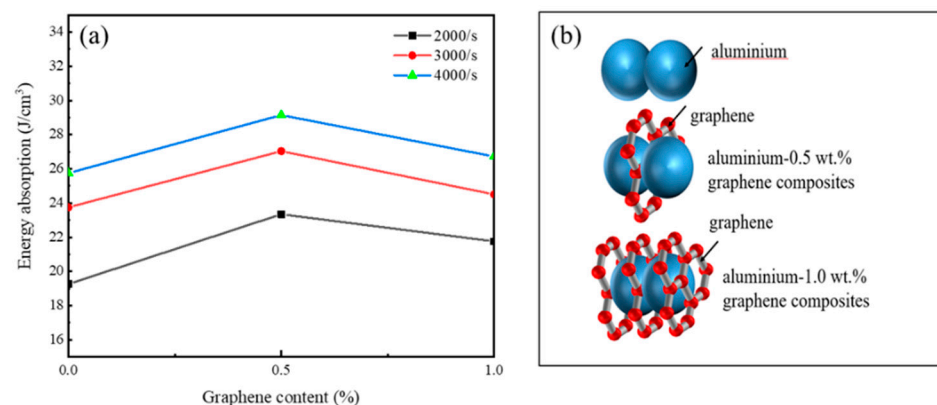


Figure 7. Aluminium–graphene absorption energy and interface schematic diagram: (a) the energy absorption capacity of aluminium-graphene composites at different strain rates; (b) schematic diagram of aluminium-graphene composite interface.

Figures 8 and 9 show SEM images of the fracture surfaces of composites subjected to quasi-static compression and a high-strain-rate impact. The results show that the fracture morphology is completely different between quasi-static loading and high-strain-rate loading. There is a relationship between the fracture morphology and the strain rate. From the quasi-static compression test samples, the fracture surfaces of the pure aluminium samples in Figure 8a showed ductile damage with small cracks and therefore greater elongation. The Figure 8b,c samples of aluminium matrix composites with a graphene addition had larger fracture surfaces with brittle damage and were found to have a high density of deformation areas on the fracture surface. For the samples tested with the separate Hopkinson press bar test, the pure aluminium sample did not fracture due to the high degree of bonding between the aluminium powder particles and aluminium powder particles in it, and the sample was pressed directly into a pie shape. The other samples of the composite with graphene addition all fractured into several pieces. As can

be seen in Figure 7, the composites cracked more and more as the strain rate increased. The fracture surfaces of their composites all show brittle damage and a large number of cracks. The results show that the addition of graphene leads to brittle fractures, which justifies the schematic diagram in Figure 5b. This is due to the fact that the graphene in the aluminium matrix composite with the added graphene breaks the bond between the aluminium powder particles and the aluminium powder particles: the more graphene added, the worse the interfacial bond. The presence of the interface leads to a wave impedance at both of the interfaces and therefore results in more cracks.

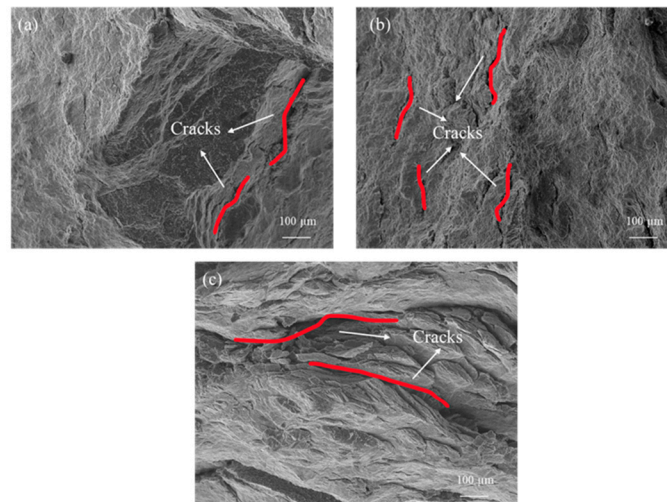


Figure 8. SEM micrograph of a fractured specimen after quasi-static loading: (a) aluminium; (b) aluminium-0.5 wt.% graphene composites; (c) aluminium-1.0 wt.% graphene composites.

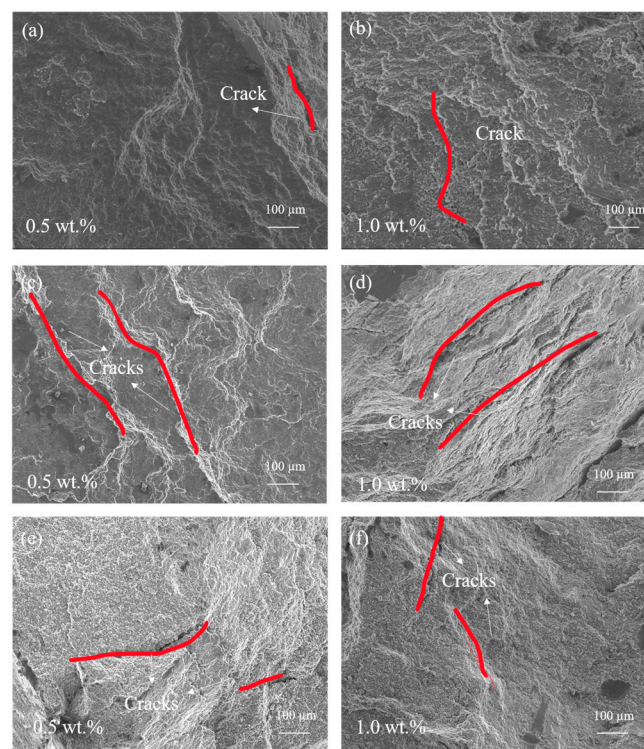


Figure 9. SEM micrographs of the fracture surfaces of the composites after SHPB tests at different strain rates: (a,b) 2000/s; (c,d) 3000/s; (e,f) 4000/s.

4. Conclusions

Aluminium–graphene composites with a uniform distribution were prepared by hot press sintering, and their compression behaviours at different strain rates were studied. The compressive stress increases with the addition of graphene up to 0.5 wt.% and then decreases with a further increase in the graphene content; however, these numbers are higher than that of a pure aluminium matrix. The maximum quasi-static and dynamic compression stresses of the aluminium-0.5 wt.% graphene composite are 238 and 299 MPa, respectively. At the same strain rate, the energy absorption capacity of the aluminium matrix increases with the addition of graphene, reaching a maximum value at 0.5 wt.% graphene. The increased performance is mainly related to the interfacial bonding strength and wave impedance between aluminium and graphene interfaces. The current research has demonstrated that aluminium-graphene composites prepared by powder metallurgical methods can be applied in dynamic impact environments with good results. However, further optimising the process is the next research priority. At present, aluminium-graphene matrix composites can be applied to the bumpers of special vehicles. This not only acts as a decoration, but it also plays an important role in absorbing and mitigating the external impact force and protecting the safety of the body and passengers. At the same time, aluminium-graphene matrix composites also meet the requirements for the lightweighting and impact resistance of small precision instruments.

Author Contributions: Y.Y.: conceptualization, validation, formal analysis, writing—original draft; J.Z.: validation, resources, conceptualization, formal analysis; L.C.: investigation, conceptualization, validation, formal analysis; H.Z.: data curation, validation, formal analysis; O.K.-K.: project administration, funding acquisition, writing—review and editing; O.V.T.: project administration, funding acquisition, writing—review and editing; F.Y.: project administration, funding acquisition; P.J.: supervision, project administration, funding acquisition, writing—review and editing; S.K.: supervision, formal analysis, writing—review and editing. All authors have read and agreed to the published version of the manuscript.

Funding: This work was supported by High-strength, high-precision, superconducting rail transit aluminum research and development and industrialization projects (2019TSLH0110), the Foundation of Strengthening Program (2019-JCJQ-142-00), Special funds for Jiangsu Provincial Science and Technology Plan in 2022 (International Science and Technology Cooperation of Innovation Support Plan/Hong Kong, Macao and Taiwan Science and Technology Cooperation) (BZ2022035), the Ministry of Science and Higher Education of the Russian Federation within the framework of the “World-class Science Center” program: Advanced digital technologies (Grant Agreement No. 075-15-2022-312 from 20 April 2022), and the Exchange Project of the Third Meeting of the Science and Technology Cooperation Subcommittee of the China-Ukraine Intergovernmental Cooperation Committee (CU03-11).

Data Availability Statement: Not applicable.

Acknowledgments: This work was supported by High-strength, high-precision, superconducting rail transit aluminum research and development and industrialization projects (2019TSLH0110), the Foundation of Strengthening Program (2019-JCJQ-142-00), Special funds for Jiangsu Provincial Science and Technology Plan in 2022 (International Science and Technology Cooperation of Innovation Support Plan/Hong Kong, Macao and Taiwan Science and Technology Cooperation) (BZ2022035), the Ministry of Science and Higher Education of the Russian Federation within the framework of the “World-class Science Center” program: Advanced digital technologies (Grant Agreement №075-15-2022-312 from 20 April 2022), and the Exchange Project of the Third Meeting of the Science and Technology Cooperation Subcommittee of the China-Ukraine Intergovernmental Cooperation Committee (CU03-11).

Conflicts of Interest: The authors declare no conflict of interest.

References

1. Chak, V.; Chattopadhyay, H.; Dora, T.L. A review on fabrication methods, reinforcements and mechanical properties of aluminum matrix composites. *J. Manuf. Process.* **2020**, *56*, 1059–1074. [\[CrossRef\]](#)
2. Güler, Ö.; Bağcı, N. A short review on mechanical properties of graphene reinforced metal matrix composites. *J. Mater. Res. Technol.* **2020**, *9*, 6808–6833. [\[CrossRef\]](#)
3. Khanna, V.; Kumar, V.; Bansal, S.A. Mechanical properties of aluminium-graphene/carbon nanotubes (CNTs) metal matrix composites: Advancement, opportunities and perspective. *Mater. Res. Bull.* **2021**, *138*, 111224. [\[CrossRef\]](#)
4. Su, J.L.; Teng, J. Recent progress in graphene-reinforced aluminum matrix composites. *Front. Mater. Sci.* **2021**, *15*, 79–97. [\[CrossRef\]](#)
5. Saboori, A.; Dadkhah, M.; Fino, P.; Pavese, M. An Overview of Metal Matrix Nanocomposites Reinforced with Graphene Nanoplatelets; Mechanical, Electrical and Thermophysical Properties. *Metals* **2018**, *8*, 423. [\[CrossRef\]](#)
6. Zhang, P.X.; Yan, H.; Wei, L.; Zou, X.L.; Tang, B.B. Effect of T6 Heat Treatment on Microstructure and Hardness of Nanosized Al₂O₃ Reinforced 7075 Aluminum Matrix Composites. *Metals* **2019**, *9*, 44. [\[CrossRef\]](#)
7. Al-Salihi, H.A.; Mahmood, A.A.; Alalkawi, H.J. Mechanical and wear behavior of AA7075 aluminum matrix composites reinforced by Al₂O₃ nanoparticles. *Nanocomposites* **2019**, *5*, 67–73. [\[CrossRef\]](#)
8. Orłowska, M.; Pixner, F.; Hütter, A.; Enzinger, N.; Olejnik, L.; Lewandowska, M. Manufacturing of coarse and ultra-fine-grained aluminum matrix composites reinforced with Al₂O₃ nanoparticles via friction stir processing. *J. Manuf. Process.* **2022**, *80*, 359–373. [\[CrossRef\]](#)
9. Ye, T.K.; Xu, Y.X.; Ren, J. Effects of SiC particle size on mechanical properties of SiC particle reinforced aluminum metal matrix composite. *Mater. Sci. Eng. A* **2019**, *753*, 146–155. [\[CrossRef\]](#)
10. Sadhu, K.K.; Mandal, N.; Sahoo, R.R. SiC/graphene reinforced aluminum metal matrix composites prepared by powder metallurgy: A review. *J. Manuf. Process.* **2023**, *91*, 10–43. [\[CrossRef\]](#)
11. Rojas, J.L.; Siva, B.V.; Sahoo, K.L.; Crespo, D. Viscoelastic behavior of a novel aluminum metal matrix composite and comparison with pure aluminum, aluminum alloys, and a composite made of Al-Mg-Si alloy reinforced with SiC particles. *J. Alloys Compd.* **2018**, *744*, 445–452. [\[CrossRef\]](#)
12. Pourmand, N.S.; Asgharzadeh, H. Aluminum Matrix Composites Reinforced with Graphene: A Review on Production, Microstructure, and Properties. *Crit. Rev. Solid State Mater. Sci.* **2019**, *45*, 289–337. [\[CrossRef\]](#)
13. Wang, Y.; Zhou, J.X.; Cheng, K.M.; Wu, J.H.; Yang, Y.S. Progress on Preparation, Microstructure and Property of Graphene Reinforced Aluminum Matrix Composite. *Mater. Sci. Forum.* **2017**, *898*, 917–932. [\[CrossRef\]](#)
14. Zhao, Z.Y.; Bai, P.K.; Du, W.B.; Liu, B.; Pan, D.; Das, R.; Liu, C.T.; Guo, Z.H. An overview of graphene and its derivatives reinforced metal matrix composites: Preparation, properties and applications. *Carbon* **2020**, *170*, 302–326. [\[CrossRef\]](#)
15. Wang, J.; Guo, L.N.; Lin, W.M.; Chen, J.; Liu, C.L.; Chen, S.D.; Zhang, S.; Zhen, T.T. Effect of the graphene content on the microstructures and properties of graphene/aluminum composites. *New Carbon Mater.* **2019**, *34*, 275–285. [\[CrossRef\]](#)
16. Kwon, H.; Mondal, J.; AlOgab, K.A.; Sammelselg, V.; Takamichi, M.; Kawaski, A.; Leparoux, M. Graphene oxide-reinforced aluminum alloy matrix composite materials fabricated by powder metallurgy. *J. Alloys Compd.* **2017**, *698*, 807–813. [\[CrossRef\]](#)
17. Zaiemyek, Z.; Liaghat, G.H.; Ahmadi, H.; Khan, M.K.; Razmkhah, O. Effect of strain rate on deformation behavior of aluminum matrix composites with Al₂O₃ nanoparticles. *Mater. Sci. Eng. A* **2019**, *753*, 276–284. [\[CrossRef\]](#)
18. Wang, M.J.; Shen, J.H.; Chen, B.; Wang, Y.F.; Umeda, J.; Kondoh, K.; Li, Y.L. Compressive behavior of CNT-reinforced aluminum matrix composites under various strain rates and temperatures. *Ceram. Int.* **2022**, *48*, 10299–10310. [\[CrossRef\]](#)
19. Wang, Z.W.; Guo, Z.Y.; Yan, Y.F.; Liu, Y.; Han, S.B.; Ji, P.G.; Yunusov, F.A.; Tolochko, O.V.; Yin, F.X. Preparation of lightweight glass microsphere/Al sandwich composites with high compressive properties. *Mater. Lett.* **2022**, *308*, 131220. [\[CrossRef\]](#)
20. Khanna, V.; Kumar, V.; Bansal, S.A. Effect of reinforcing graphene nanoplatelets (GNP) on the strength of aluminum (Al) metal matrix nanocomposites. *Mater. Today Proc.* **2022**, *61*, 280–285. [\[CrossRef\]](#)
21. Sharma, A.; Vasudevan, B.; Sujith, R.; Kotkunde, N.; Suresh, K.; Gupta, A.K. Effect of Graphene Nanoplatelets on the Mechanical Properties of Aluminium Metal Matrix Composite. *Mater. Today Proc.* **2019**, *18*, 2461–2467. [\[CrossRef\]](#)
22. Zhang, B.Y.; Lin, Y.F.; Zhai, D.X.; Wu, G.H. Quasi-static and high strain rates compressive behavior of aluminum matrix syntactic foams. *Compos. Part B-Eng.* **2016**, *98*, 288–296. [\[CrossRef\]](#)
23. Lin, Y.F.; Zhang, Q.; Ma, X.Y.; Wu, G.H. Mechanical behavior of pure Al and Al-Mg syntactic foam composites containing glass cenospheres. *Compos. Part A Appl. Sci. Manuf.* **2016**, *87*, 194–202. [\[CrossRef\]](#)
24. Gao, Y.B. Preparation of Graphene-Reinforced Aluminium Matrix Composites and Study of Their Properties. Master's Thesis, North Central University, Taiyuan, China, 2019.

Disclaimer/Publisher's Note: The statements, opinions and data contained in all publications are solely those of the individual author(s) and contributor(s) and not of MDPI and/or the editor(s). MDPI and/or the editor(s) disclaim responsibility for any injury to people or property resulting from any ideas, methods, instructions or products referred to in the content.